

Date: August 21, 2023

Department of Translational Molecular Pathology (TMP)

Immune Profiling Laboratory

Cancer Immune Monitoring and Analysis Center

The University of Texas MD Anderson Cancer Center

TMP-Immunoprofiling (TMP-IL) Laboratory Director:

Cara Haymaker, Assistant Professor, TMP

Immunohistochemistry and Digital Pathology Lab Director:

Luisa Maren Solis Soto, TMP, Assistant Professor, TMP

THE UNIVERSITY OF TEXAS

**MD Anderson
Cancer Center**

Making Cancer History®

NanoString GeoMx Digital Spatial Profiling Analytical Validation of Immuno-oncology Protein Targets

1. Technical platform

The GeoMx® Digital Spatial Profiling (DSP) technology is a novel platform developed by nanoString. This product relies upon antibodies coupled to photocleavable oligonucleotide tags. After the incubation of antibodies to slide-mounted tissue sections, cell types of interest with fluorescent morphology markers to create fluorescent images for selecting region of interest (ROIs). The oligonucleotide tags are released from discrete regions of the tissue via UV exposure. Released tags are quantitated in an nCounter® and counts are mapped back to tissue location, yielding a spatially resolved digital profile of analyte abundance (1). Antibodies used in this panel have been validated by vendor and the validation is available in the following website [WP_GeoMx_Antibody_Validation_White_Paper.pdf \(nanostring.com\)](http://www.nanostring.com/WP_GeoMx_Antibody_Validation_White_Paper.pdf)

This document describes **verification and validation** of the **assay performance** that have been performed at the Translational Molecular Pathology Immunoprofiling laboratory (TMP-IL). A smooth workflow and standard of operating procedures are developed by our laboratory (2).

2. Analytes

- a. *GeoMx DSP Morphology Biomarkers for Visualization of Solid Tumor and Tumor Microenvironment:*

PanCK, CD45, SYTO13

PanCK, CD3, CD68, SYTO13

- b. *GeoMx Human Immuno-Oncology Protein Assays(3)*

• Immune Cell Profiling Core: Beta-2-microglobulin; CD3; CD56; CTLA4; GZMB; PD-1; CD11c; CD4; CD68; Pan-cytokeratin; HLA-DR; PD-L1; CD20; CD45; CD8; Fibronectin; Ki-67; SMA; Negative controls (Ms IgG2a, Ms IgG1, and Rb IgG); Positive controls (S6, Histone H3 and GAPDH).

• IO Drug Target Module: 4-1BB; LAG3; ARG1; OX40L; B7-H3; STING; GITR; TIM-3; IDO1; VISTA.

• Immune Activation Status Module: CD127; CD25; CD27; CD40; CD44; CD80; ICOS; PD-L2.

• Immune Cell Typing Module: CD14; CD163; CD34; CD45RO; CD66b; FAPalpha; FOXP3.

3. Analytical characteristics

nanoString GeoMx Digital Spatial profiler platform	
Parameters	Normalized DSP counts of the GeoMx Human Immuno-Oncology Protein Assay obtained from regions of interest of up to 660 μm x 785 μm guided by morphological assessment of formalin fixed paraffin embedded (FFPE) tissue.
Accuracy	Accuracy was measured by the capacity of the assay to accurately identify known biological compartments (Germinal center, Interfollicular area, Mantle zone) in reactive tonsil tissue using differentially expressed biomarkers in specific regions of interest and unsupervised hierarchical cluster analysis; and for the capacity of the assay to identify known targets in specific biological compartments of lung adenocarcinoma tumor tissue (Tumor, T-cell, Macrophage compartment). Refer to "4. Validation of biological correlates and differential protein expression", "5. Validation of DSP biomarkers using targeted compartment segmentation", and "6. Inter-run reproducibility of biological validation results and inter-run reproducibility of DSP assay"
Analytical sensitivity	Analytical sensitivity was measured by the capacity of the assay to detect known differentially expressed biomarkers in each biological compartment in reactive tonsil tissue. Refer to "4. Validation of biological correlates and differential protein expression"
Analytical specificity	Analytical specificity was determined by using an orthogonal platform (single chromogenic immunohistochemistry) of a set of 27 biomarkers included in the panel; and the data obtained from multiplex immunofluorescence of 3 targets with corresponding DSP counts. Refer to "8. Validation of GeoMx DSP biomarkers using single chromogenic Immunohistochemistry" and "10. Correlation of biomarker quantification obtained from multiplex immunofluorescence and DSP counts"
Precision Inter-assay and intra-assay reproducibility.	Inter-assay reproducibility was measured by testing three different runs, on different days and different operators. Intra-assay reproducibility was measured by testing 2 different assays on the same day and with the same operator. Refer to "8. Validation of GeoMx DSP biomarkers using single chromogenic Immunohistochemistry", "9. Reproducibility of DSP counts obtained in FFPE multi-tissue TMA" and "7. Intra-run reproducibility of DSP assay"
Establishment of appropriate quality control & improvement procedures	Positive and negative controls are included in the GeoMx Human Immuno-Oncology Protein Assays. All the required equipment has annual service contracts with regular Preventive Maintenance performed to maintain optimal calibration and performance. All other small equipment and laboratory material have calibration performed by certified vendors.

4. Validation of biological correlates of differential protein expression

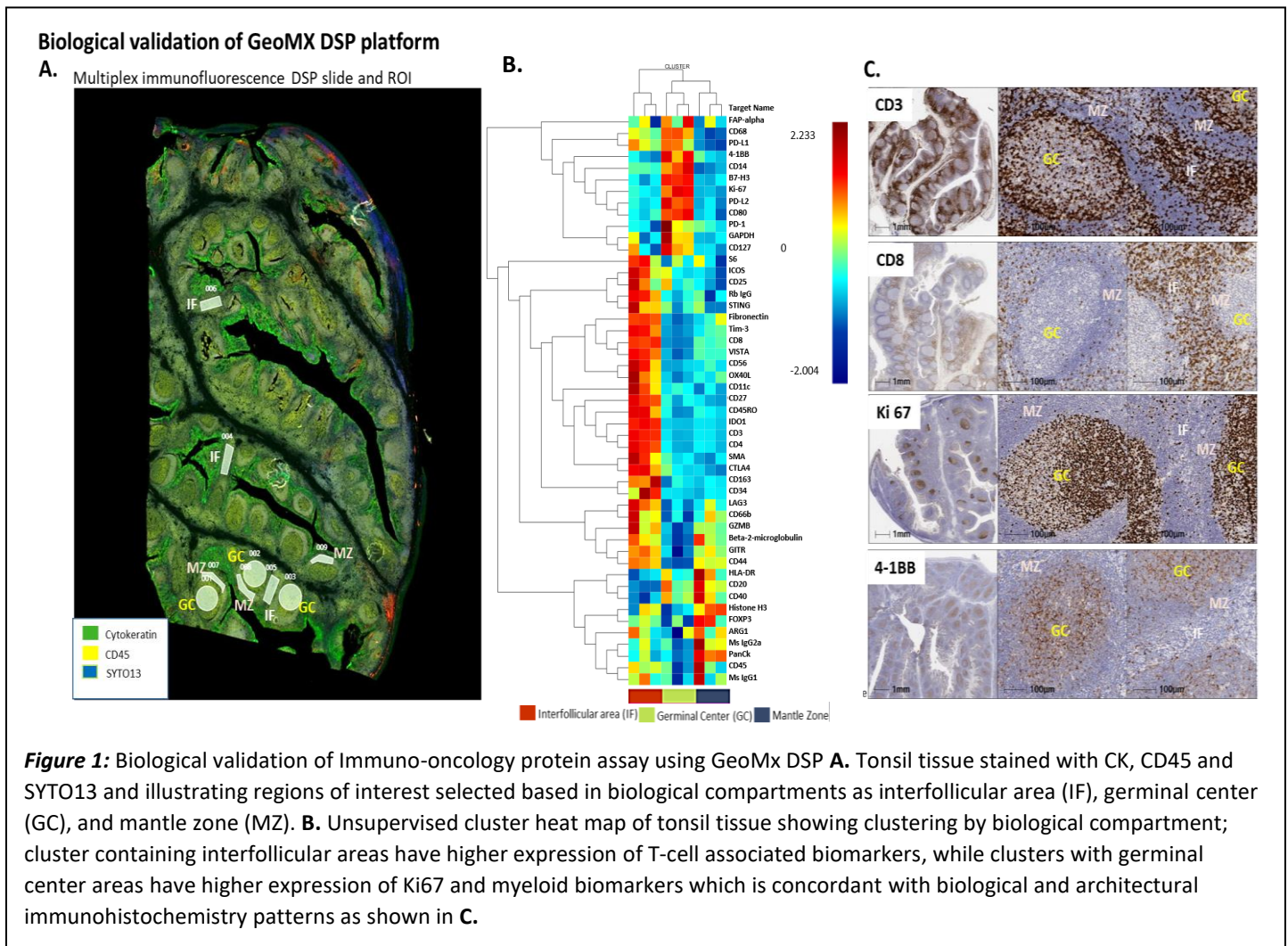
First, we used a formalin fixed-paraffin embedded (FFPE) reactive tonsil tissue processed with the GeoMx DSP assay to evaluate the expression of biomarkers in different biological compartments defined as: Germinal center (GC), Interfollicular areas (IF) and Mantle zones (MZ). Then, we evaluated if the biomarkers differentially expressed on those compartments are concordant to known biological and immunohistochemistry patterns.

Experimental Design

Samples: One 5µm section of FFPE with reactive tonsil tissue.

Selection of Regions of Interest. We selected three regions of interest (ROIs) placed in each biological compartment for a total of 9 ROI (GC, 3; IF, 3; MZ, 3) **Figure 1A**. Placement of ROI was guided by morphology evaluation of the multiplex immunofluorescence (mIF) imaged section, performed by a pathologist.

Data quality control and normalization: We used the GeoMx DSP analysis software for data quality control, normalization and statistical analysis (4). After quality control of the DSP data obtained and mapped to ROI, the data was normalized using housekeeper proteins. We performed an unsupervised cluster heatmap and identified biomarkers with higher expression in each cluster (**Figure 1B**).



Results: The cluster heatmap showed that the ROI clustered in concordance with each biological compartment **Figure 1.A**. Then, we interrogated which biomarkers were differentially expressed in the profiled biological compartments. We found that biomarkers expressed by T-cell such as CD3, CD4 and CD8 in the interfollicular area have higher DSP counts compared to germinal center and mantle zone; while Ki67, and biomarkers expressed in myeloid cells were higher in the germinal center compared to interfollicular and mantle areas. These results are concordant with biological and architectural pattern observed by immunohistochemistry. **Table 1, Figure 1 C.**

<i>Germinal Center compared to Interfollicular area</i>			<i>Interfollicular area compared to Mantle zone</i>			<i>Germinal Center Compared to Mantle Zone</i>		
Target name	Log2	P value	Target name	Log2	P value	Target name	Log2	P value
CD3	-3.0832	0.0037	CD3	2.8819	0.0042	CD44	-2.4858	0.0052
CD8	-3.3207	0.0011	CD8	1.9724	0.0006	CD8	-1.3483	0.0028
CD4	-2.1519	0.0080	CD4	2.0187	0.0102	CD80	1.0959	0.0007
CD44	-3.1036	0.0100	CD27	1.2460	0.0024	B7-H3	1.1784	0.0002
IDO1	-2.9943	0.0029	Tim-3	1.0749	0.0128	CD68	1.2707	0.0010
VISTA	-2.0656	0.0062	CTLA4	1.5517	0.0201	PD-L1	1.3588	0.0282
CD45RO	-1.7441	0.0259	CD45RO	1.4553	0.0384	PD-L2	2.1512	0.0136
Tim-3	-1.6188	0.0126	CD14	1.0486	0.0017	Ki-67	2.1899	0.0188
CTLA4	-1.1573	0.0200	PD-L1	1.1781	0.0345	CD14	2.5994	0.0376
CD56	-1.1463	0.0423	VISTA	1.2807	0.0145			
CD27	-1.0926	0.0015	IDO1	2.8246	0.0028			
B7-H3	1.1362	0.0019						
4-1BB	1.1692	0.0159						
Ki-67	1.7837	0.0204						
PD-L2	1.7872	0.0187						

Table 1. Differential expressed biomarkers by biological compartments

* Statistical analysis was performed in the GeoMx DSP analysis software, we used a non-paired T-test, and plotted the data in a Volcano plot. A fold change greater than 1 and lower than -1, and a p value ≤ 0.005 were used as cutoff for statistical significance.

In addition, we quantified the percentage of tissue area with immunohistochemistry protein expression of selected IHC biomarker (CD3, CD8, Ki67, 4-1BB) in tonsil tissue, in specific areas representing each biological compartment (germinal center, Interfollicular and mantle zone) using digital image analysis (Halo, Indica lab). Then we calculated the fold-change of IHC expression of these biomarkers between the compartments. Log2 fold-change (log2FC) is determined by taking the ratio of the mean of the percentage of protein expression for IHC and the normalized protein counts for DSP, followed by a log2 transformation to obtain a normal or near-normal distribution. We found similar fold-changes of protein expression for both assays (**Table 2**) with coefficient of variations lower than 2.3% (**Table 3**). Of note the biological compartments displayed similar cell densities of the areas of analysis, therefore the data was not further divided in subsets based on cellularity.

	KI67		CD3		CD8		4-1BB	
	IHC	DSP	IHC	DSP	IHC	DSP	IHC	DSP
<i>Germinal Center compared to Interfollicular area</i>	2.94	1.78	-1.31	-3.08	-4.08	-3.32	4.06	1.16
<i>Germinal Center Compared to Mantle Zone</i>	2.84	2.18	0.51	-0.20	-2.57	-1.34	2.90	0.98
<i>Interfollicular area compared to Mantle zone</i>	-0.09	0.40	1.82	2.88	5.84	1.97	-1.15	-0.18

Table 2. Differential expressed biomarkers by biological compartments (log2FC) for IHC and DSP assay.

	GC n/mm2	IF n/mm2	Mantle n/mm2
Number of values	3	3	3
Minimum	10320	12386	10259
Maximum	10788	12538	10711
Range	468.1	152.0	451.7
Mean	10541	12453	10523
Std. Deviation	235.2	77.36	235.4
Std. Error of Mean	135.8	44.66	135.9
Coefficient of variation	2.231%	0.6212%	2.237%

Table 3. Descriptive statistics of cellularity by area of analysis.

5. Validation of DSP biomarkers using targeted compartment segmentation

To assess the expression of DSP protein biomarkers in compartments segmented by mIF protein expression, we used annotated DSP data from a cohort of FFPE lung adenocarcinoma assayed with GeoMx Digital Spatial Profiling (DSP) protein protocol with morphology markers that targeted Epithelial (panCK), T cells (CD3) and macrophage (CD68) and the same immune-oncology DSP panels (49 immune biomarkers)

Experimental design

Samples: Thirty-three FFPE lung adenocarcinoma tumor tissue were placed in two tissue microarray (1-mm core in triplicate) from the MD Anderson ICON cohort.

Segmentation strategy: Pancytokeratin (panCK; Tumor), CD3 (T cell), CD68 (Macrophage) and SYTO 13 (nuclear) were utilized as morphology biomarkers. Regions of interests (up to 660x785um) were placed in cores containing tumor and segmented in biological compartments: "Tumor" (PanCK+), "T cell enriched" (CD3+) and "Macrophage enriched" (CD68+).

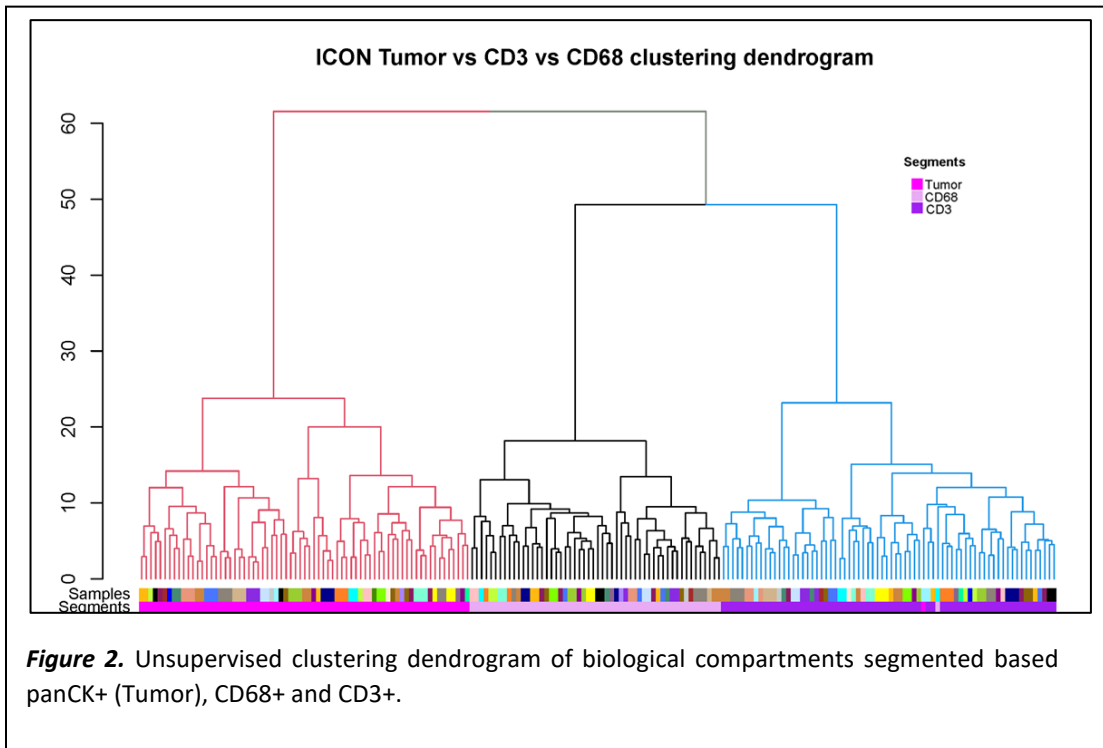


Figure 2. Unsupervised clustering dendrogram of biological compartments segmented based on panCK+ (Tumor), CD68+ and CD3+.

Results:

After DSP normalization, an unsupervised clustering dendrogram was performed. As shown in **Figure 2**, three main clusters were obtained that aligned with the biological compartments of Tumor, CD3+, and CD68+ as shown in **Figure 2**.

A Mann Whitney U test was used to evaluate the differences between the biological compartments.

Adjusted p values ≤ 0.05 and Log₂ fold changes of ≥ 1 and ≤ -1 were considered statistically significant.

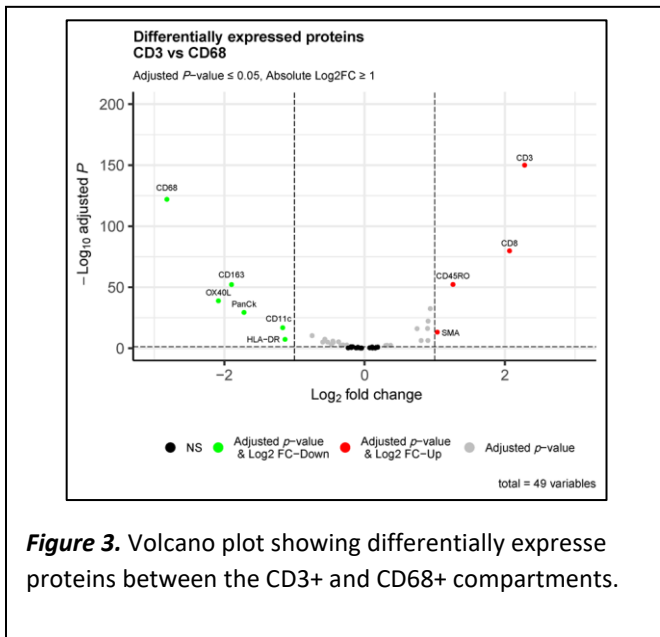


Figure 3. Volcano plot showing differentially expressed proteins between the CD3+ and CD68+ compartments.

Differentially expressed proteins between CD3+ and CD68+ compartments: We observed upregulation of CD3, CD8, SMA (smooth muscle actin) and CD45RO in the CD3+ compartment, when compared to the CD68+ compartment; while, the latter showed upregulation of CD68, CD163, OX40L, panCK, HLA-DR and CD11c (Figure 3) compared to CD3+ compartment. These results are in concordance with known biomarker expression in T-cell and myeloid cells respectively. Of note panCK expression in CD68+ compartment maybe related to higher vicinity of tumor cells to macrophages.

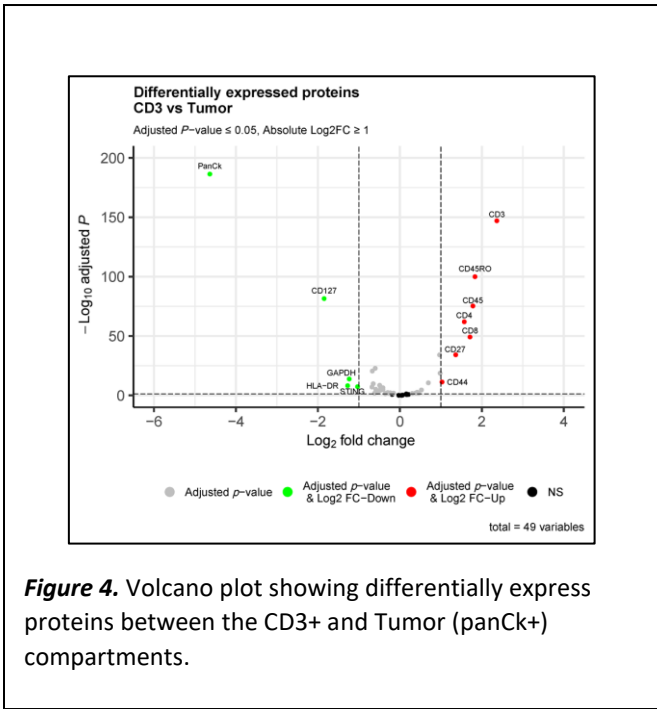


Figure 4. Volcano plot showing differentially expressed proteins between the CD3+ and Tumor (panCK+) compartments.

Differentially expressed proteins between CD3+ and Tumor (panCK+) compartments:

We observed upregulation of CD3, CD8, CD45, CD4, CD27, CD44 and CD45RO in the CD3+ compartment, when compared to the Tumor compartment; while, the latter showed upregulation of panCK, CD127, HLA-DR and STING (**Figure 4**) compared to CD3+ compartment. These results are in concordance with known biomarker expression in T-cell and carcinoma cells respectively.

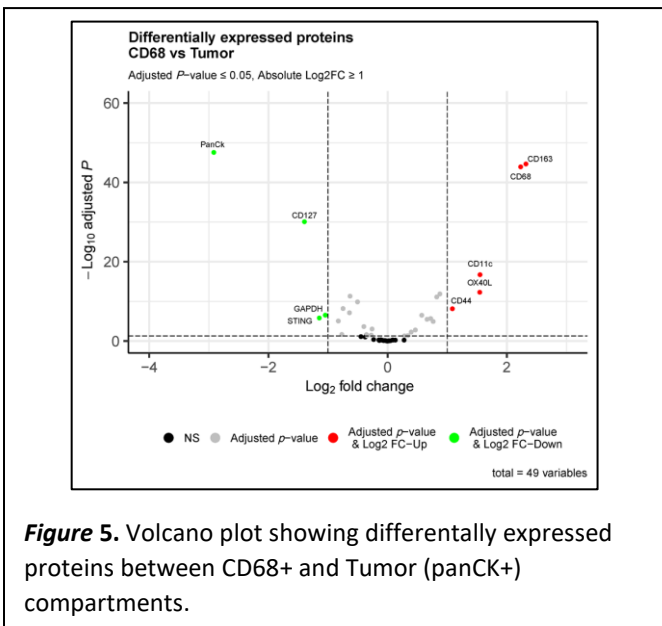


Figure 5. Volcano plot showing differentially expressed proteins between CD68+ and Tumor (panCK+) compartments.

Differentially expressed proteins between CD68+ and Tumor (panCK+) compartments:

We observed upregulation of CD163, CD68, CD11c, OX4-L and CD44 in the CD68+ compartment, when compared to the Tumor compartment; while, the latter showed upregulation of panCK, CD127, GAPDH and STING (**Figure 5**) compared to CD68+ compartment. These results are in concordance with known biomarker expression in myeloid cells and carcinoma cells respectively.

6. Inter-run reproducibility of biological validation results and inter-run reproducibility of DSP assay

To investigate reproducibility of the assay in two independent tests at separate times (Test 1, day 1; and Test 2, more than 2 months apart), we replicated the analysis using a different section of the same reactive tonsil tissue and similar strategy for ROI selection.

Experimental design

Samples: One 5µm section of FFPE with reactive tonsil tissue.

ROI selection strategy: We placed 3 ROI in each biological compartment (GC, IF, MZ) identified by morphological assessment of the mIF image. Of note, ROI did not match the exact spatial area of previous slide since the serial section did not exhibit the same biological compartments.

Data quality control and normalization: The data was normalized using housekeeping proteins after quality control.

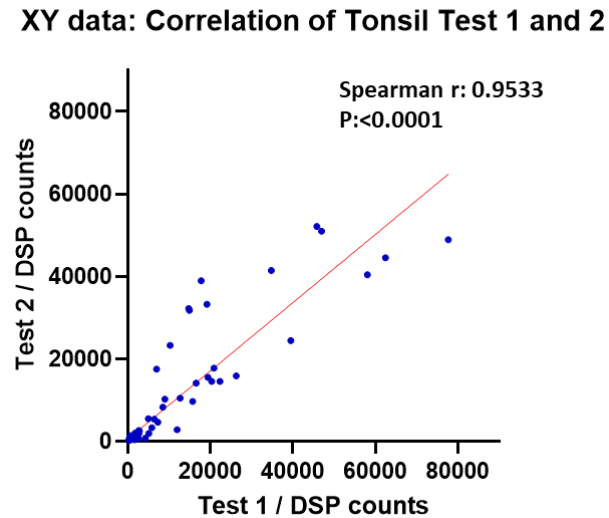
Results: Like previous analysis, the unsupervised cluster analysis heatmap showed that the data clustered according to the defined biological compartments. The statistical analysis showed that the biomarkers in **Table 4** were differentially expressed in both reactive tonsil tissues ($r \geq 0.5$; $p \leq 0.05$).

Then we correlated the data obtained from both tests using the average of DSP counts of ROI category (GC, IF, Mantle). for each tonsil, the corresponding result showed a significant positive correlation. **Figure 6**

<i>Tonsil Test 1 and Test 2</i>		
<i>Germinal Center compared to Interfollicular area</i>	<i>Interfollicular area compared to Mantle zone</i>	<i>Germinal Center Compared to Mantle Zone</i>
CD3	CD3	CD80
CD8	CD8	CD68
Ki-67	CD4	PD-L1
CD56	ID01	PD-L2
CD4	CD27	Ki-67
VISTA	Tim-3	CD127
Tim-3	VISTA	
PD-L2		
CD44		

Table 4. Differential expressed biomarkers by biological compartments shared in both tonsil tests (Test 1 and Test 2)

Figure 6 Spearman correlation of GeoMx DSP counts of protein targets obtained from two non-serial sections of same tonsil specimen, more than 2 months apart (Test 1 and Test 2), using average of DSP counts of matched biological regions of interest (Germinal Center, Mantle and Interfollicular area). Data was normalized by housekeepers



7. Intra-run reproducibility of DSP assay

To test the intra-run reproducibility of the assay, we performed DSP assay in 2 serial sections that belong to the lung cancer TMA block in the same day, and time. Then we correlated the data by DSP counts and individual biomarkers.

Experimental design

Samples: 16 FFPE lung adenocarcinoma tumor tissue was placed in two tissue microarray (1-mm core) from the MD Anderson ICON cohort. We performed the GeoMx Digital Spatial Profiling (DSP) protein protocol to assess the 49 immune biomarkers.

Segmentation strategy: Pancytokeratin (panCK; epithelial), CD3 (T cell), CD68 (Macrophage) and SYTO 13 (nuclear) were utilized as morphology biomarkers. Regions of interests (up to 660x785um) were placed in cores containing tumor and segmented in biological compartments: “Tumor” (PanCK+) and “TME” (panCK-)

Statistical analysis: Data was normalized by Housekeepers and correlations were analyzed using the Spearman correlation method.

Results

For both Tumor and TME segments, all the correlation values showed a p value of less than 0.05 (**Table 5a and 5b**) (**Figure7**). Please see appendix attached.

Tumor	R	p-value
Number of values (46)		
Minimum	0.4152	1.790e-031
25% Percentile	0.7364	3.410e-019
Median	0.8357	3.480e-012
75% Percentile	0.9210	9.460e-009
Maximum	0.9793	0.004572
Range	0.5642	0.004572
Mean	0.7966	0.0002283
Std. Deviation	0.1535	0.0008496
Std. Error of Mean	0.02263	0.0001239
Coefficient of variation	19.27%	372.2%

TME	R	p-value
Number of values (46)		
Minimum	0.3091	6.790e-025
25% Percentile	0.6785	2.465e-017
Median	0.8103	8.150e-011
75% Percentile	0.9107	1.195e-006
Maximum	0.9627	0.04369
Range	0.6536	0.04369
Mean	0.7760	0.001090
Std. Deviation	0.1623	0.006440
Std. Error of Mean	0.02393	0.0009496
Coefficient of variation	20.91%	590.9%

Table 5a. Descriptive statistics of correlation R and p values from tumor.

Table 5b. Descriptive statistics of correlation R and p values from TME

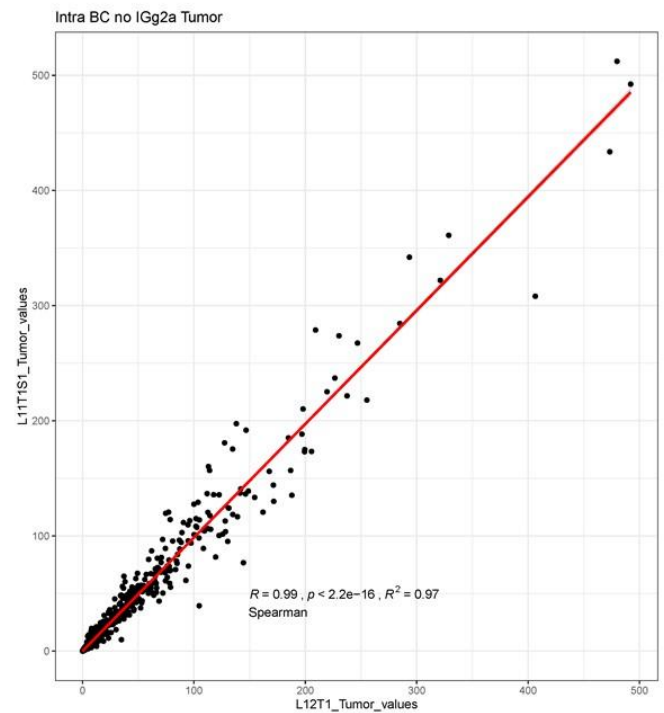
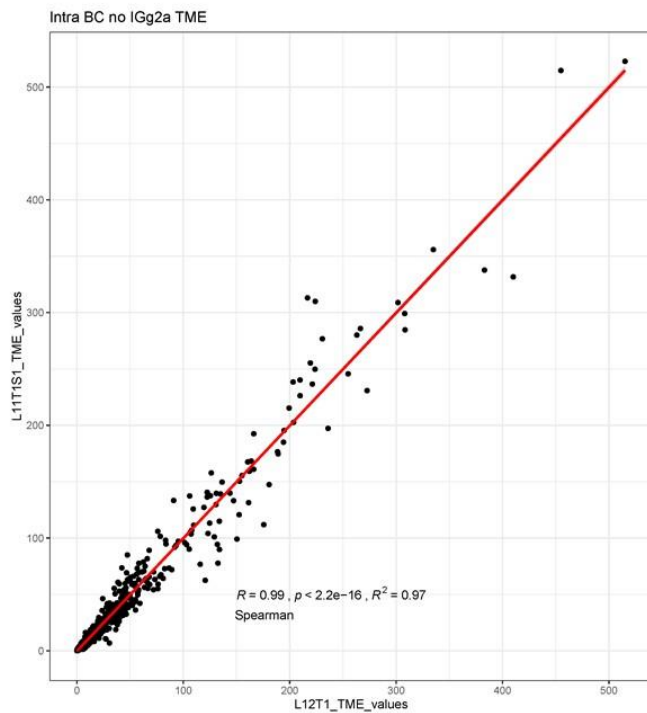


Figure 7. Correlation plots for TME and Tumor segments from the intra-run assay.

8. Validation of GeoMx DSP biomarkers using single chromogenic Immunohistochemistry

To further validate the Immune oncology panels of the GeoMx DSP assay and to compare outputs with standard immunohistochemistry, we used FFPE tissue controls including normal and tumoral tissue placed in a tissue microarray (TMA), and we stained them with both GeoMx DSP assay and a set of 27 IHC biomarkers that were previously optimized in the TMP-IL laboratory.

Experimental design

Samples:

- i. One 5 µm section of FFPE multi-tissue TMA. The TMA was built using 1-mm cores of the following tissue
 - Spleen (3 cores)
 - Hodgkin lymphoma (3 cores)
 - Pancreas (3 cores)
 - Tonsil (9 cores)
 - Placenta (6 cores)
 - Glioblastoma multiforme (3 cores)
 - Ovarian carcinoma (3 cores)
 - Colorectal carcinoma (3 cores)
 - Melanoma (3 cores)
 - Lymph node (3 cores)
 - Liver (3 cores)
 - Cell blocks of Tumor infiltrating Lymphocytes (3 cores)
 - Cell blocks of PBMCs (Peripheral Blood Mononuclear Cells) (3 cores)
- ii. One 5 µm section of FFPE Tonsil tissue

GeoMx DSP analysis:

ROI selection strategy: In the FFPE TMA slide, we placed one ROI of up to 660 µm x 785 µm on each core of the FFPE TMA. We avoided necrosis, tissue folds, and artifacts **Figure 8 A**. In the reactive tonsil tissue slide, we selected three ROI of up to 660x785 µm placed in each biological compartment (GC, IF, MZ) for a total of 9 ROIs.

Data quality control and normalization: The data was QC'ed and normalized using background correction and housekeeper proteins. We extracted normalized DSP counts for further statistical analysis.

Immunohistochemistry (IHC) analysis and Scoring:

We used Leica Bond automated stainer to perform IHC staining in 5 µm section of FFPE with the following antibodies optimized at TMP-IL: Arginase 1, CD3, CD11c, CD14, CD20, CD44, CD45, CD45RO, CD163, CD8, Foxp3, HLA-DR, IDO1, Ki67, panCK, PD-L1, Sting, B2-Microglobulin, B7-H3, CD4, CD56, CD137, ICOS, PD-1, TIM-3, LAG3 and VISTA **Table 6**.

Antibody	Clone	Vendor	Dilution factor
Arg1	D4E3M	Cell Signaling Technology	1:400
CD3	D7A6E	Cell Signaling Technology	1:200
CD11c	EP1347Y	Abcam	1:800
CD14	SP192	Abcam	1:400
CD20	L-26	DAKO	1:1400
CD44	EPR18668	Abcam	1:6000
CD45	EP322Y	Abcam	1:200
CD45RO	T200-797	Abcam	1:2000
CD163	10D6	Leica	1:200
CD8	C8/144B	ThermoFisher	1:25
Foxp3	206D	BioLegend	1:50
HLA-DR	EPR3692	Abcam	1:500
IDO1	D5J4E	Cell Signaling Technology	1:400
Ki67	MIB-1	DAKO	1:100
panCK	AE1/AE3	DAKO	1:50
PD-L1	E1L3N	Cell Signaling Technology	1:100
Sting	pAb	ProteinTech	1:1000
B2-Microglobulin	D8P1H	Cell Signaling Technology	1:1000
B7-H3	D9M2L	Cell Signaling Technology	1:80
CD4	EPR6855	Abcam	1:200
CD56	EP2567Y	Abcam	1:50
CD137	D2Z4Y	Cell Signaling Technology	1:50
ICOS	D1K2T	Cell Signaling Technology	1:100
PD-1	EPR 4877(2)	Abcam	1:250
TIM-3	D5D5R	Cell Signaling Technology	1:100
VISTA	D1L2G	Cell Signaling Technology	1:200
LAG3	D2G50	Cell Signaling Technology	1:100

Table 6. Information of antibodies used by single chromogenic immunohistochemistry.

Scoring: We scan all IHC slides at 20x using Aperio AT2 scanner (Leica Biosystem). We used Halo digital image analysis software (Indica Lab) to visualize and perform digital image analysis. First, we selected matched areas selected for DSP analysis **Figure 8 B**. We avoided necrosis, tissue folds and artifacts. We used the quantification

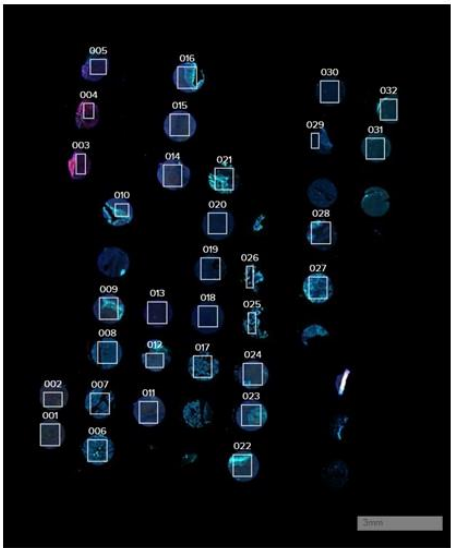
algorithm to quantify percentage of area with positive expression **Figure 8 C**. We exported the results for further statistical analysis.

Results

Figure 8 Microphotographs illustrating regions of interest (ROI) selection in multiplex (mIF) DSP slide in **A**, and immunohistochemistry (IHC) in **B**. **C** shows IHC expression of CD11c and corresponding digital image analysis to evaluate percentage of positive staining to illustrate digital image analysis strategy.

Validation of biomarkers of GeoMx DSP platform using IHC analysis in a multitissue TMA

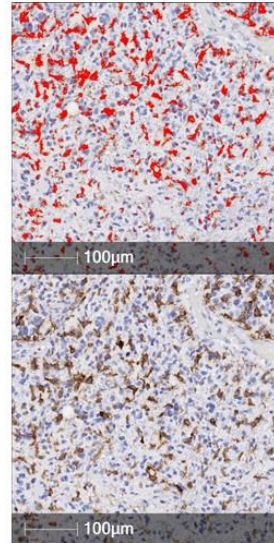
A. mIF DSP slide and ROI selection



B. IHC slide and ROI selection



C. Image analysis of IHC slides



Correlation of GeoMx DSP counts and IHC scoring: We correlated normalized DSP counts and results obtained from IHC analysis performed using Digital image analysis software for each core and each biomarker; the results accounted for different methods of quantification, including 1. extension, 2. percentage of positive cells, 3. cell density and 4. intensity of positive staining. They were expressed as: 1. % of positive area (percentage of positive staining of the entire ROI analyzed), 2. % of positive cells (percentage of positive cells from the total cells within the ROI), Avg stain OD (the average optical density of the positive stain in the entire ROI) and positive cell density (number of positive cells per square mm in the whole ROI), respectively. We found a positive correlation with Spearman $r \geq 0.4$, and p value < 0.05 for 20 biomarkers with at least one method of quantification and at least one method of normalization (Housekeeper or background correction) (**Table 7**).

	% positive area				% positive cells				Avge Stain OD				Positive cell density			
	DSP Norm HK		DSP Norm BC		DSP Norm HK		DSP Norm BC		DSP Norm HK		DSP Norm BC		DSP Norm HK		DSP Norm BC	
	Spearman r	P values	Spearman r	P values	Spearman r	P values	Spearman r	P values	Spearman r	P values	Spearman r	P values	Spearman r	P values	Spearman r	P values
B7H3	0.263	0.204	0.238	0.253	0.291	0.158	0.307	0.135	0.596	0.002	0.653	0.000	0.227	0.275	0.239	0.251
Arg1	0.565	0.012	0.289	0.229	0.384	0.104	0.091	0.710	0.404	0.087	0.023	0.926	0.404	0.087	0.128	0.601
B2M	0.030	0.893	0.234	0.282	-0.219	0.315	0.218	0.317	0.050	0.819	0.455	0.029	0.007	0.975	0.085	0.700
CD3	0.629	0.011	0.809	0.000	0.538	0.034	0.744	0.001	0.450	0.082	0.685	0.004	0.612	0.014	0.785	0.001
CD4	0.329	0.125	0.100	0.650	0.375	0.078	0.228	0.295	0.392	0.064	0.301	0.162	0.175	0.425	0.195	0.373
CD8	0.442	0.021	0.291	0.141	0.432	0.025	0.090	0.656	-0.337	0.086	0.349	0.075	0.495	0.009	0.288	0.146
CD11c	0.604	0.008	0.738	0.000	0.269	0.280	0.719	0.001	0.199	0.428	0.697	0.001	0.453	0.059	0.732	0.001
CD14	0.569	0.037	0.613	0.022	0.530	0.054	0.560	0.040	0.604	0.025	0.648	0.014	0.376	0.186	0.336	0.240
CD20	0.838	0.000	0.797	0.000	0.779	0.001	0.767	0.001	0.868	0.000	0.794	0.000	0.767	0.001	0.756	0.001
CD44	0.479	0.062	0.526	0.038	0.332	0.208	0.256	0.338	0.435	0.094	0.406	0.120	-0.032	0.908	-0.029	0.917
CD45	0.795	0.000	0.881	0.000	0.796	0.000	0.899	0.000	0.785	0.000	0.903	0.000	0.805	0.000	0.896	0.000
CD45RO	0.290	0.180	0.436	0.038	0.256	0.239	0.431	0.040	0.298	0.167	0.412	0.051	0.240	0.270	0.410	0.052
CD56	0.397	0.049	0.334	0.103	0.496	0.012	0.329	0.108	0.448	0.025	0.274	0.185	0.297	0.149	0.325	0.113
CD163	0.625	0.001	0.665	0.000	0.625	0.001	0.671	0.000	0.616	0.001	0.642	0.001	0.609	0.001	0.668	0.000
ICOS	0.066	0.764	0.238	0.274	0.034	0.879	0.170	0.438	0.167	0.446	0.222	0.308	0.048	0.826	0.231	0.288
FOXP3	-0.076	0.773	-0.022	0.936	0.268	0.297	0.386	0.127	0.365	0.150	0.566	0.020	0.174	0.502	0.322	0.207
HLA-DR	0.682	0.001	0.884	0.000	0.726	0.000	0.894	0.000	0.564	0.008	0.822	0.000	0.713	0.000	0.904	0.000
IDO1	0.542	0.027	0.652	0.006	0.532	0.030	0.600	0.012	0.564	0.020	0.645	0.006	0.505	0.041	0.561	0.021
Ki67	0.841	0.000	0.906	0.000	0.853	0.000	0.962	0.000	0.885	0.000	0.947	0.000	0.897	0.000	0.912	0.000
LAG3	-0.162	0.471	-0.151	0.503	-0.152	0.499	-0.079	0.728	-0.259	0.244	-0.204	0.362	-0.217	0.333	-0.159	0.480
PD-L1	0.598	0.002	0.448	0.025	0.642	0.001	0.451	0.024	0.297	0.149	0.222	0.287	0.638	0.001	0.492	0.012
panCK	0.547	0.046	0.477	0.087	0.530	0.054	0.451	0.108	0.560	0.040	0.477	0.087	0.525	0.057	0.442	0.116
PD1	0.045	0.828	-0.174	0.395	0.069	0.736	0.167	0.414	-0.154	0.452	-0.019	0.925	0.090	0.662	-0.143	0.485
STING	0.504	0.028	0.696	0.001	0.588	0.008	0.795	0.000	0.614	0.005	0.793	0.000	0.507	0.027	0.581	0.009
TIM3	0.178	0.395	0.189	0.365	0.122	0.560	0.145	0.490	0.171	0.414	0.262	0.207	0.129	0.538	0.126	0.548
VISTA	-0.196	0.420	-0.009	0.972	-0.182	0.455	-0.153	0.533	-0.116	0.637	-0.179	0.464	-0.177	0.468	-0.007	0.977
41BB	-0.080	0.710	-0.014	0.949	-0.054	0.802	0.032	0.881	-0.410	0.047	-0.155	0.470	-0.084	0.695	0.047	0.828

Table 7. Correlation of normalized DSP counts and results obtained from IHC analysis performed using Digital image analysis software.

Then, we stained with single IHC the biomarkers with a poorest correlation, specifically: B2-microglobulin, B7-H3, CD4, CD56, 4-1BB, ICOS, PD-1, TIM-3, LAG3 and VISTA, and performed digital image analysis in similar areas selected in the DSP assay in tonsil tissue.

The results showed that IHC data have positive correlation with corresponding DSP counts for CD4 (r , 0.85; p , 0.0061) and B7H3 (r , 0.7; p , 0.0433). VISTA, ICOS, TIM3 and 4-1BB have a positive correlation with $r \geq 0.4$, but a p value >0.05 . The following biomarkers: B2-microglobulin, LAG3 and PD1 did not have significant positive correlation in any of our analysis. This may be due to lack of appropriate negative and positive controls that could allow us to obtain a wider range of expression for correlation analysis. Besides, serial sections may not be representative of the same levels of expression in IHC and DSP due to heterogeneity of expression intrinsic of these tissues.

To further study the effect of differences of cellularity of the tissue types in the correlation of biomarkers, we separated the samples into high cellularity “Lymphoid” tissue (spleen, Hodgkin lymphoma, tonsil and lymph node) and low cellularity “Solid” tissue (pancreas, placenta, Glioblastoma, ovarian carcinoma, Colorectal carcinoma, melanoma and liver). First, we evaluated if this classification in fact corresponded to high and low cellularity tissue, we used a T test non-paired statistical analysis to compare total cell densities (n/mm²) obtained from cell segmentation analysis of DSP assay (total cells/surface area); we found a significant difference between the tissue types, tissues classified as “solid” has lower cell densities (median, 3774 cells/mm²) compared to “lymphoid” tissue (median 13750 cells/mm²) (**Figure 9**).

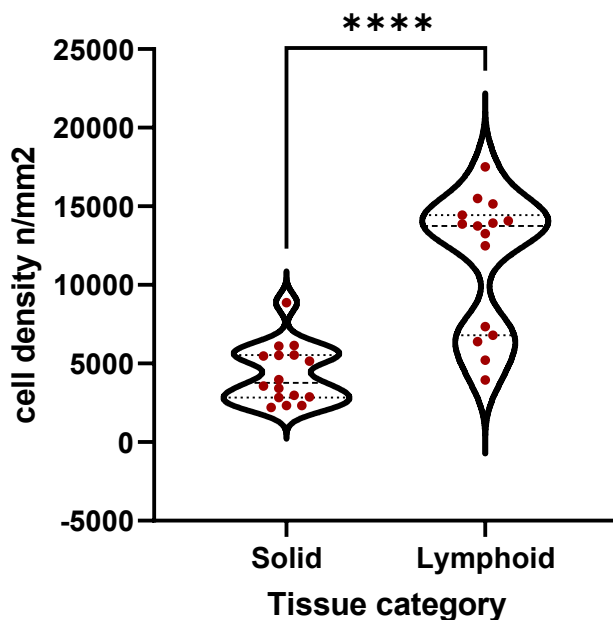


Figure 9. Violin plot showing differences of the distribution of cell density values in tissue classified as “solid” and “lymphoid” cell densities. **** p value <0.0001 .

Then, we performed correlations between DSP counts of each biomarker normalized by housekeepers and background correction, by these categories (“lymphoid” and “solid”). For most of the biomarkers, no correlation was found in these categories. However, for a subset of the biomarkers, the correlation was maintained or higher in lymphoid tissue category (CD163 and CD20) or in solid tissue category (Arg1, CD163, CD56, Ki67, PanCK, PD-L1, STING). These findings are most likely related to the range of the expression of these biomarkers in these specific tissue categories, further

analysis in a large sample size is needed to infer proper biological conclusions. (**Table 8a and 8b**).

Biomarker normalized by Housekeepers	Lymphoid tissue		Solid tissue	
	P values	Spearman r	P values	Spearman r
41-BB	0.0876	-0.5455	0.3063	0.3077
Arg1	0.1938	0.4833	0.0369	0.7167
B2 -miroglobulin	0.4918	-0.2485	0.7784	-0.0879
B7-H3	0.9739	0.0140	0.7506	0.0989
CD11c	0.4483	0.2727	0.6646	0.1905
CD14	0.7833	-0.2000	0.0666	0.6500
CD163	0.0306	0.6636	0.0473	0.5659
CD20	0.0083	0.8333	0.2000	0.5714
CD3	0.9349	0.0476	0.0576	0.7143
CD4	0.3415	0.3182	0.6673	0.1399
CD44	0.5008	0.2857	0.1389	0.6429
CD45	0.6436	0.1833	0.1548	0.4909
CD45RO	0.4348	-0.3182	0.1546	0.4636
CD56	0.3415	-0.3182	0.0061	0.7308
CD8	0.0591	0.5664	0.1408	0.4000
Foxp3	0.0544	0.6364	0.6583	0.2571
HLA-DR	0.4101	-0.3167	0.0839	0.5245
ICOS	0.3304	-0.3455	0.4434	0.2448
IDO-1	0.4697	0.2606	0.1028	0.7714
KI67	0.0694	0.6905	0.0000	1.0000
LAG3	0.1955	-0.3846	0.8574	0.0330
PanCK	0.5948	0.2500	0.0238	0.8571
PD1	0.8861	-0.0490	0.3436	0.3297
PD-L1	0.1457	-0.4727	0.0153	0.6440
STING	0.9460	0.0303	0.0279	0.7857
TIM-3	0.1217	0.5000	0.6595	0.1297
VISTA	0.2957	-0.3697	0.8801	-0.0667

Table 8a: Correlations between DSP results normalized by housekeepers, per biomarker by tissue category, “lymphoid” and “solid”.

Biomarker normalized by Background correction	Lymphoid tissue		Solid tissue	
	P values	Spearman r	P values	Spearman r
41-BB	0.1546	0.4636	0.3734	-0.2692
Arg1	0.7081	-0.1500	0.0968	0.6000
B2 -miroglobulin	0.8916	0.0545	0.9929	0.0055
B7-H3	0.9910	-0.0070	0.5911	0.1648
CD11c	0.0734	0.6000	0.0154	0.8333
CD14	0.3500	0.6000	0.1618	0.5167
CD163	0.0033	0.8182	0.1517	0.4231
CD20	0.0083	0.8333	0.4976	0.3214
CD3	0.3268	0.4048	0.0962	0.6429
CD4	0.5393	0.2091	0.2869	-0.3357
CD44	0.2431	0.4762	0.0480	0.7857
CD45	0.0255	0.7500	0.2325	0.4182
CD45RO	0.5765	0.1636	0.6937	-0.1364
CD56	0.8603	0.0636	0.0741	0.5165
CD8	0.6192	0.1608	0.9949	-0.0036
Foxp3	0.0072	0.8061	0.5639	0.3143
HLA-DR	0.1618	0.5167	0.0009	0.8462
ICOS	0.6073	0.1879	0.5280	-0.2028
IDO-1	0.1334	0.5152	0.2972	0.5429
KI67	0.1323	0.5952	0.0022	0.9286
LAG3	0.6428	0.1429	0.5073	-0.0659
PanCK	0.9063	0.0714	0.0238	0.8571
PD1	0.7493	-0.1049	0.7506	0.0989
PD-L1	1.0000	0.0000	0.6706	0.1253
STING	0.9184	0.0424	0.0004	0.9762
TIM-3	0.0519	0.6091	0.3176	0.2879
VISTA	0.6073	-0.1879	0.9116	0.0500

Table 8b: Correlations between DSP results normalized by background correction, per biomarker by tissue type “lymphoid” and “solid”

9. Reproducibility of DSP counts obtained in FFPE multi-tissue TMA

To investigate reproducibility of the assay in three independent DSP runs at different time points, and different operators. We replicated the analysis using different sections of the same FFPE multi-tissue TMA with a similar strategy for ROI selection at independent runs.

Experimental Design

Samples: One 5µm sections of FFPE multi-tissue TMA for each test:

TMA test 1: week 1/day 1 (operator 1)

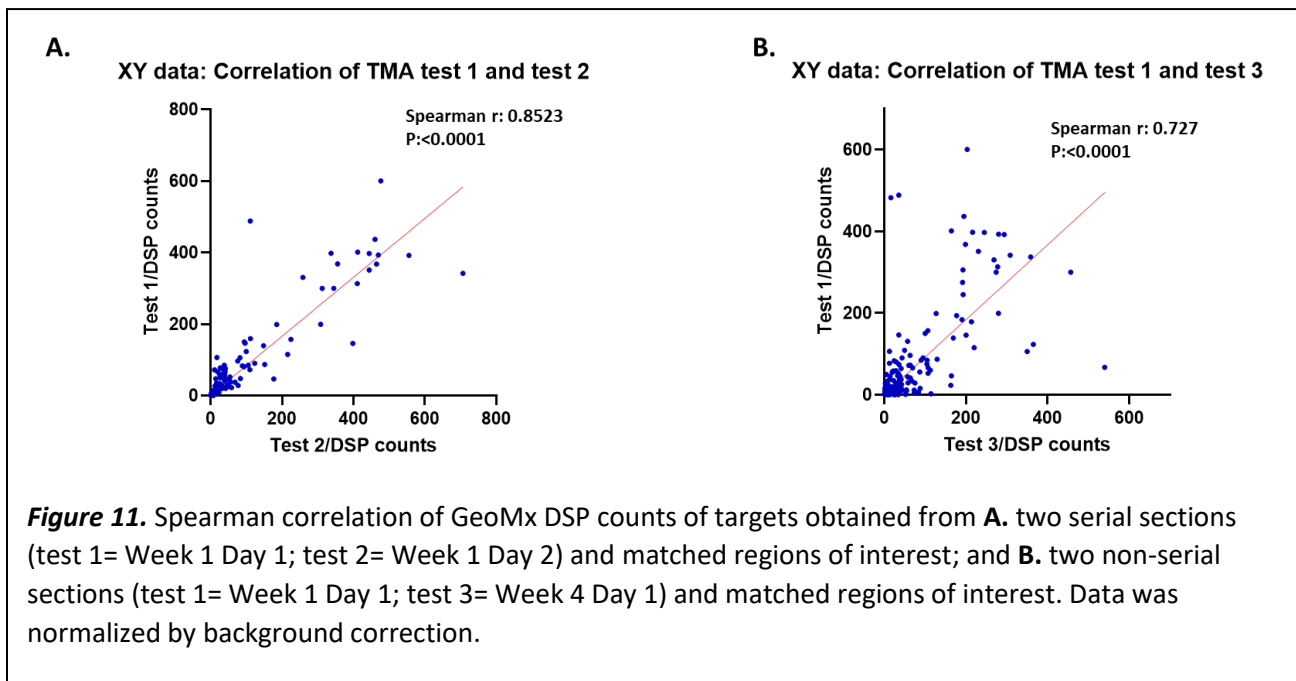
TMA test 2: week 1, day 2 (operator 1)

TMA test 3: week 4 day 1 (operator 2)

ROI selection strategy: We placed one ROI of up to 660 μm x 785 μm sections of FFPE multi-tissue TMA.

Data analysis: The data was normalized using background correction after quality control.

Results: We correlated the data obtained from TMA test 1 vs TMA test 2 and TMA test 1 and TMA test 3 using the DSP counts of each ROI, the corresponding result showed a strong positive correlation with a Spearman $r > 0.7$ and a p value < 0.001 for both tests **Figure 11**.



To further analyze the variability of expression of biomarkers, we separated the data by tissue type and performed a new correlation analysis in the following subsets: Spleen, Hodgkin lymphoma, Pancreas, tonsil, Placenta, Glioblastoma multiforme, Ovarian carcinoma, Colorectal carcinoma, Melanoma, Lymph node and Liver. We found a positive correlation for all tissue subsets. **(Figure 12, Table 10)**

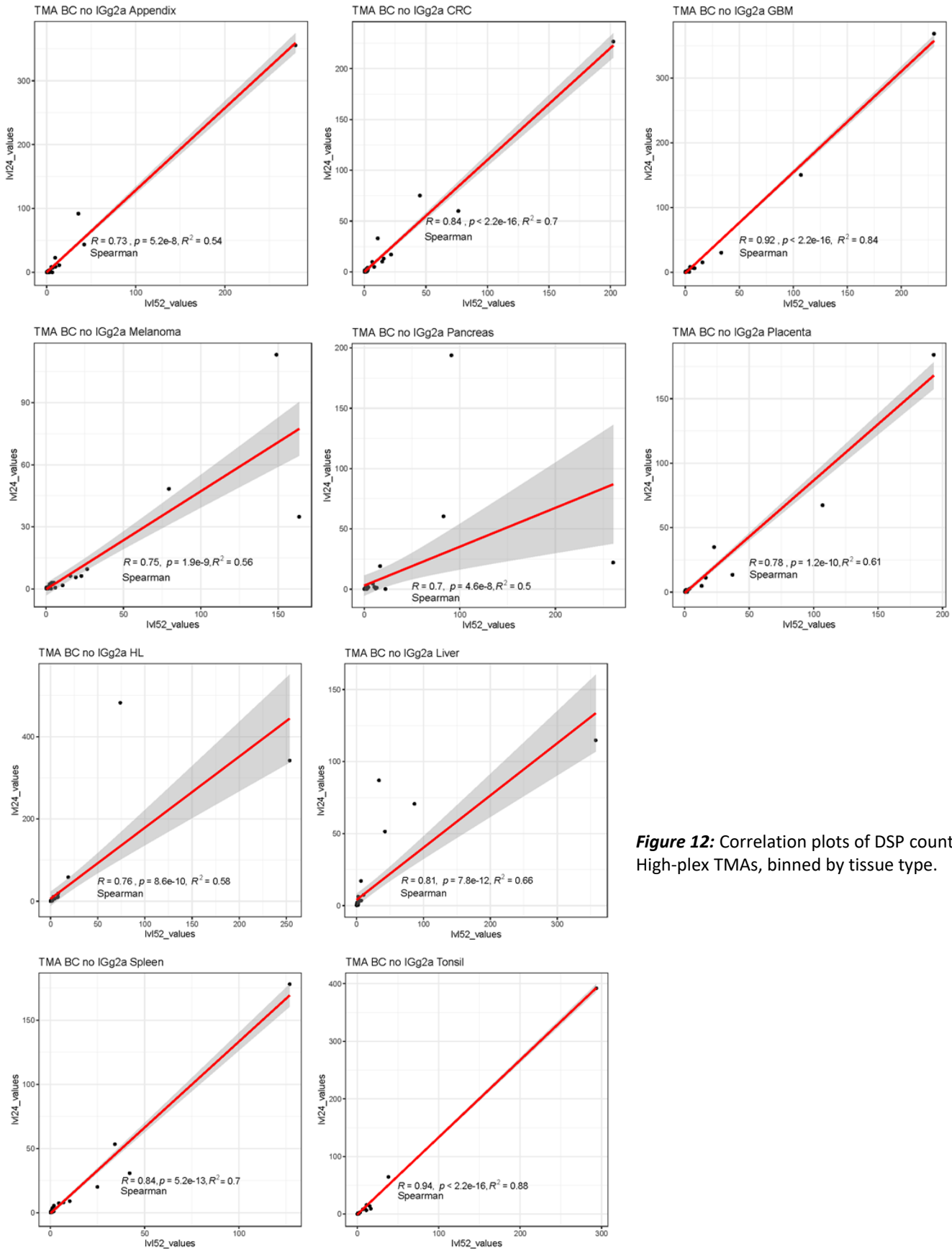


Figure 12: Correlation plots of DSP counts from 2 High-plex TMAs, binned by tissue type.

Tissue type	R	P value	R2	Lower (95% CI)	Upper (95% CI)
Pancreas	0.7	<0.001	0.5	0.520817	0.825946
Appendix	0.73	<0.001	0.54	0.563954	0.844425
Melanoma	0.75	<0.001	0.56	0.58895	0.854835
Hodgkin Lymphoma (HL)	0.76	<0.001	0.58	0.603708	0.860883
Placenta	0.78	<0.001	0.61	0.638695	0.874936
Liver	0.81	<0.001	0.66	0.682011	0.891799
Colorectal carcinoma (CRC)	0.84	<0.001	0.7	0.72583	0.908286
Spleen	0.84	<0.001	0.7	0.71953	0.90595
Glioblastoma (GBM)	0.92	<0.001	0.84	0.853666	0.953349
Tonsil	0.94	<0.001	0.88	0.885734	0.963996

Table 10: Correlation data including spearman R, p values and confidence intervals of DSP counts from 2 High-plex TMAs, binned by tissue type.

10. Correlation of biomarker quantification obtained from multiplex immunofluorescence and DSP counts:

To further evaluate performance of the assay, we evaluated biomarker expression obtained by multiplex immunofluorescence and compared it with the results obtained by the DSP protein assay. We used the multiplex immunofluorescence slide of the DSP assay performed in two TMA from the MD Anderson ICON Cohort and correlated with the corresponding DSP counts. The slides stained with morphology markers Syto 13 (nuclear), CD3, CD68 and PanCK were used to perform digital image analysis, using HALO software (Indica Lab); we estimated cell density, % of positive cells, and average intensity of CD3, CD68 and PanCK in the same regions used for DSP assay, these results were correlated with corresponding DSP counts obtained after normalization. **(Table 9a, 9b and 9c) (Figure 10).**

	Spearman R				p value			
	CK cell density n/mm2	% CK Positive Cells	CK Avg Cell Intensity	DSP panCK counts	CK cell density n/mm2	% CK Positive Cells	CK Avg Cell Intensity	DSP panCK counts
CK Cell density n/mm2	1.0000	0.9555	0.8460	0.7568		<0.0001	<0.0001	<0.0001
% CK Positive Cells	0.9555	1.0000	0.9094	0.7918	<0.0001		<0.0001	<0.0001
CK Avg Cell Intensity	0.8460	0.9094	1.0000	0.8639	<0.0001	<0.0001		<0.0001
DSP panCK counts	0.7568	0.7918	0.8639	1.0000	<0.0001	<0.0001	<0.0001	

Table 9a: Correlation of CK immunofluorescence digital image analysis data with CK DSP counts.

	Spearman R				p value			
	CD3 cell density n/mm2	% CD3 Positive Cells	CD3 Avg Cell Intensity	DSP CD3 counts	CD3 cell density n/mm2	% CD3 Positive Cells	CD3 Avg Cell Intensity	DSP CD3 counts
CD3 cell density n/mm2	1.0000	0.9961	0.7728	0.5887		<0.0001	<0.0001	<0.0001
% CD3 Positive Cells	0.9961	1.0000	0.7704	0.5754	<0.0001		<0.0001	<0.0001
CD3 Avg Cell Intensity	0.7728	0.7704	1.0000	0.5535	<0.0001	<0.0001		<0.0001
DSP CD3 counts	0.5887	0.5754	0.5535	1.0000	<0.0001	<0.0001	<0.0001	

Table 9b: Correlation of CD3 immunofluorescence digital image analysis data with CD3 DSP counts.

	Spearman R				p value			
	CD68 cell density n/mm2	% CD68 Positive Cells	CD68 Avg Cell Intensity	DSP CD68 counts	CD68 cell density n/mm2	% CD68 Positive Cells	CD68 Avg Cell Intensity	DSP CD68 counts
CD68 cell density n/mm2	1.0000	0.9915	0.5516	0.2664		<0.0001	<0.0001	0.0014
% CD68 Positive Cells	0.9915	1.0000	0.5317	0.2622	<0.0001		<0.0001	0.0016
CD68 Avg Cell Intensity	0.5516	0.5317	1.0000	0.2145	<0.0001	<0.0001		0.0104
DSP CD68 counts	0.2664	0.2622	0.2145	1.0000	0.0014	0.0016	0.0104	

Table 9c: Correlation of CD68 immunofluorescence digital image analysis data with CD68 DSP counts.

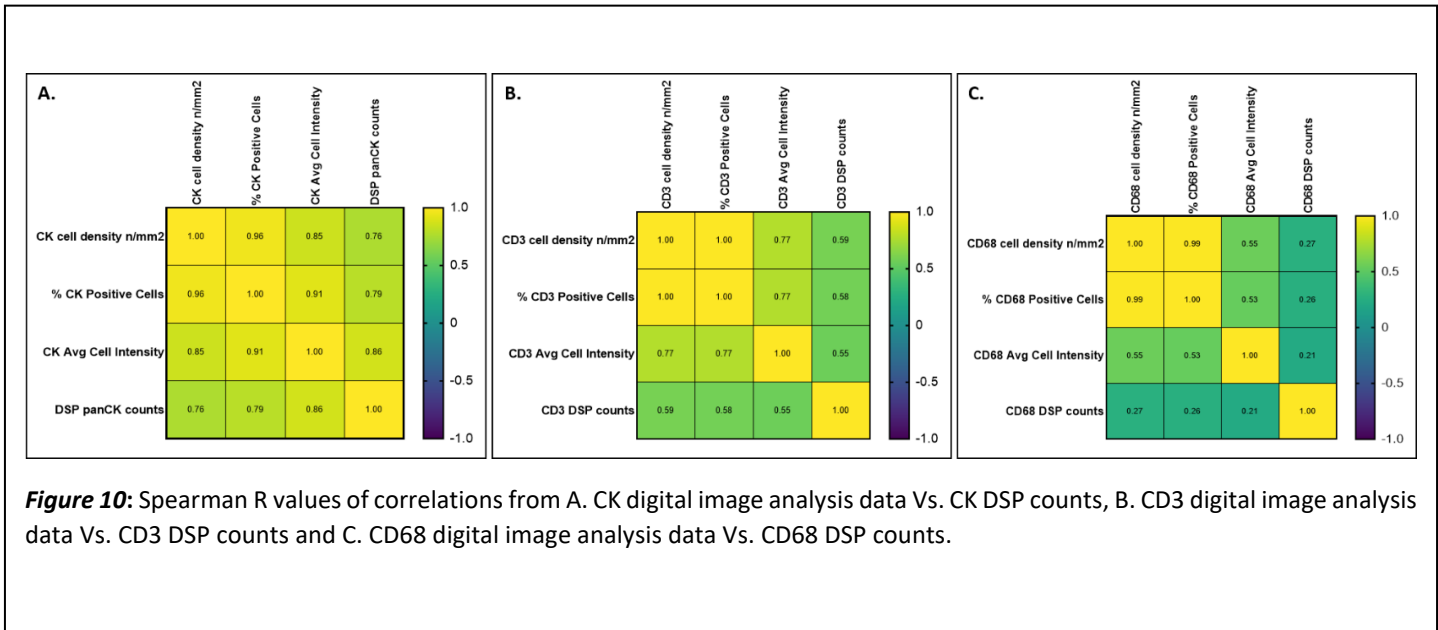


Figure 10: Spearman R values of correlations from A. CK digital image analysis data Vs. CK DSP counts, B. CD3 digital image analysis data Vs. CD3 DSP counts and C. CD68 digital image analysis data Vs. CD68 DSP counts.

Conclusion

In conclusion, our data indicates that the biomarker expression of targets included in the immune-oncology protein assay of the GeoMx DSP platform are concordant with biological and immunohistochemistry patterns observed in reactive tonsil tissue controls and multi-tissue TMA. Correlation of biomarker expression of GeoMx DSP assay and immunohistochemistry was at moderate to strong level for most biomarkers evaluated. We also observed high reproducibility among runs at the same and different run times.

References

1. Van TM, Blank CU. A user's perspective on GeoMx™ digital spatial profiling. *Immuno-Oncology Technology*. 2019;1:11-8.
2. Hernandez S, Lazcano R, Serrano A, Powell S, Kostousov L, Mehta J, et al. Challenges and Opportunities for Immunoprofiling Using a Spatial High-Plex Technology: The NanoString GeoMx(®) Digital Spatial Profiler. *Front Oncol*. 2022;12:890410.
3. NanoString I. GeoMx® Protein Assays for Immuno-Oncology 2021 [cited 2022 09/05/2022]. Available from: [chrome-extension://efaidnbmnnnibpcajpcglclefindmkaj/https://nanosttring.com/wp-content/uploads/PB_MK3350_DSP_IO_Protein_PB_R28.pdf](https://nanosttring.com/wp-content/uploads/PB_MK3350_DSP_IO_Protein_PB_R28.pdf).
4. NanoString I. MAN-10109-01 GeoMxDSPExampleDataAnalysis 2019 [cited 2022 09/05/2022]. Available from: [chrome-extension://efaidnbmnnnibpcajpcglclefindmkaj/https://nanosttring.com/wp-content/uploads/MAN-10109-01_GeoMx_DSP_Example_Data_Analysis.pdf](https://nanosttring.com/wp-content/uploads/MAN-10109-01_GeoMx_DSP_Example_Data_Analysis.pdf).

Immunohistochemistry and Digital pathology Laboratory

GeoMx DSP scientist leads:

Sharia Hernandez, MD, Research scientist.

Wei Lu, MD, PhD Principal Research scientist.

Director: Luisa Maren Solis Soto, MD Assistant Professor MD Anderson Cancer Center

Signature (Luisa M. Solis Soto)

Date: 08/12/2023